Biomass Conversion and Biorefinery
https://doi.org/10.1007/s13399-022-02324-4

ORIGINAL ARTICLE

Recycling of Labada (*Rumex*) biowaste as a value-added biosorbent for rhodamine B (Rd-B) wastewater treatment: biosorption study with experimental design optimisation

Zeynep Mine Şenol[1] · Serap Çetinkaya[2] · Hasan Arslanoglu[3]

Received: 12 November 2021 / Revised: 3 January 2022 / Accepted: 5 January 2022

Abstract
Rhodamine B (Rd-B) is a highly toxic dye causing serious environmental and health issues. This study focussed on the development of a cost-effective and ecologically friendly remediation technique utilising Labada (*Rumex*), a readily available agricultural biowaste. Experimental design was applied for the first time to establish the parametric effects on the rhodamine B (Rd-B) biosorption and to optimise the process for the highest rhodamine B (Rd-B) removal. At the optimised conditions of 25 °C, 500 mg L^{-1} concentration, natural solution pH of 5.5–6.0, and 1 g L^{-1} dosage; the maximum biosorption capacity was 0.219 mol kg^{-1}. Using the results of physicochemical characterisation and rhodamine B (Rd-B) adsorption measurements, isotherm and kinetic models were made to predict performance towards rhodamine B (Rd-B) removal from water reliably. The rhodamine B (Rd-B) biosorption kinetic was best correlated to the pseudo-second-order, while the equilibrium to the Freundlich isotherm. These isotherm and kinetic models can be used to quickly screen among larger sets of possible adsorbents and guide the development of novel, highly efficient adsorbents for rhodamine B (Rd-B) removal from water. Characterisation of Labada (*Rumex*) was accomplished by scanning electron microscope (SEM–EDX), energy dispersive X-ray, Fourier transform infrared, and thermogravimetric analyses. Regeneration of exhausted Labada (*Rumex*) biosorbent was best performed using 50% hydrochloric acid. This study highlights the strong feasibility of Labada (*Rumex*) biosorption as a green and effective technique for Rd-B removal.

Keywords Rhodamine B (Rd-B) · Labada (*Rumex*) · Experimental design · Regeneration

Highlight
- Extensive use of dyes is resulting in their accumulation in the environment.
- Labada (Rumex) were used for rhodamine B (Rd-B) removal from water.
- Effective reduction of the treated water samples was achieved.

✉ Hasan Arslanoglu
hasan.arslanoglu@comu.edu.tr

Zeynep Mine Şenol
msenol@cumhuriyet.edu.tr

Serap Çetinkaya
secetinkaya@cumhuriyet.edu.tr

[1] Zara Vocational School, Department of Food Technology, Cumhuriyet University, Sivas, Turkey

[2] Department of Molecular Biology and Genetics, Faculty of Science, Cumhuriyet University, Sivas, Turkey

[3] Faculty of Engineering, Department of Chemical Engineering, Çanakkale Onsekiz Mart University, Çanakkale, Turkey

1 Introduction

Over the last number of years, the unprecedented increase in water pollution due to discharge of dyes from various industries such as paper, textile, paints, and cosmetics has been highlighted as a major problem. This arising threat bears harmful consequences for freshwater ecosystems. The current global worth of colorant market amounting to 32 billion USD is expected to rise to 42 billion USD soon. Annually, 700,000 t of synthetic dyes are produced while 15% of dyes discharged in water are toxic and xenobiotic [1]. Enrichment of dyes in water prevents photosynthesis process and limits the microbial activity of water plants [18]. Coagulation, ultrafiltration, adsorption, biodegradation, photochemical, and flocculation methodologies have been adopted to extract dye effluents [5]. The main concern is generation of toxic by-products generated by frequent applications of these methods for wastewater remediation [21].

Published online: 14 January 2022

Conventional methods for the treatment of textile industry wastewater include the principle of decolorisation and reduction of organic matter. Although most of the pollutants other than paint can be removed by chemical and physical methods, various physical/chemical methods such as flocculation/coagulation, adsorption, and chemical oxidation and biological treatment methods can be used for dye removal from wastewater. Although ozone, hydrogen peroxide (H_2O_2), Fenton reagent, UV/H_2O_2, chlorination, ultrafiltration, and electrochemical methods have very high colour removal efficiency; they are very expensive methods. Biological methods are known to be insufficient for colour removal due to the resistance of dyestuffs to biodegradation [16]. Textile wastewater is classified as wastewater that is difficult to treat due to the different chemicals it contains and especially the dyestuffs in question [26].

In recent years, adsorption has been used as an effective method for removing the colour of textile dyes, but it is not preferred because it is expensive. Therefore, low-cost and effective materials are being developed. Sugarcane, natural clay, sunflower, sepiolite, fly ash, montmorillonite and sepiolite, natural zeolite, orange peel, and date cluster are adsorbents used for the removal of dyes from wastewater [20, 28]. The widespread use of dyes resulting in increased depletion in nature poses a threat to non-target species, including humans, to flora and fauna. Therefore, efficient removal strategies are essential and adsorption used in the literature seems to be the simplest approach in this sense [7, 27].

Labada (*Rumex*) is a genus of plants containing about 200 annual, biennial, and perennial plant species. The leaves of non-sour species are widely consumed in Anatolia by wrapping and are used as efelik, evelik etc. while the sour-leaved species are called sorrel. Members of this family are perennial plants that are very common, often grown in the northern hemisphere, but spread everywhere. Some are weeds, and some are grown for their edible leaves. Labada species are used as food by the larvae of many butterfly species. However, the Labada (*Rumex*) pods are inedible, and these are discarded as solid biowaste. For agricultural waste minimisation and wastewater remediation purposes, it is desired to convert the Labada (*Rumex*) biowaste into value-added biosorbent for dyes removal [9].

Biosorption of dyes from aqueous media is a complex process, which depends on a number of parameters such as biosorbent dosage, solution pH, adsorption duration, system temperature, particle size, and concentration of dye ions [33]. The desired efficient removal performance can be established through optimising the process parameters. The objective of the present study was to determine the potential recycling of an agricultural biowaste, Labada (*Rumex*), as a biosorbent for rhodamine B (Rd-B) removal. The biowaste conversion into a low-cost, non-toxic, and eco-friendly biosorbent was attained without any chemical usage. Different adsorption models were used to determine the adsorption equilibrium, kinetic, and mechanisms. Lastly, a regeneration study was carried out to investigate the reusability of the spent biosorbent to ensure the economic feasibility of the developed process.

2 Materials and methods

2.1 Chemicals

Sodium hydroxide (NaOH), hydrochloric acid (HCl), and rhodamine B ($C_{28}H_{31}ClN_2O_3$, 479.02 g/gmol) were used in the experiments were of analytical purity and were obtained from Merck and Sigma-Aldrich companies.

Rhodamine B is a highly water-soluble dyestuff. Rhodamine B has amphoteric properties, although it is generally included in the dyestuff group with basic properties. Thus, the chromophore groups that give the colour of the dyestuffs form the cation group of the molecule. The auxochromes, which provide the binding tendencies of the dyestuffs, are the dimethylamino groups in the molecular. The chromophore groups of dyestuffs are linked by quinoid rings (double-bonded rings). Rhodamine B dyestuff is in the xanthene chemical group and fluorene subgroup, and two of the three aryl rings have a dimethylamino group, and one has a carboxyl group (Fig. 1) [15].

2.2 Preparation of Labada (*Rumex*).

Labada (*Rumex*) was obtained from a local market in Sivas, Turkey. The edible waste was separated from the pods. The Labada (*Rumex*) were washed multiple times with deionised water to remove dirt prior to drying at 80 °C in a forced-convection oven for 2 days. The dried Labada (*Rumex*) were cut into small pieces, followed by pulverisation in a mill. The ground Labada (*Rumex*) were sieved using a sieve shaker to

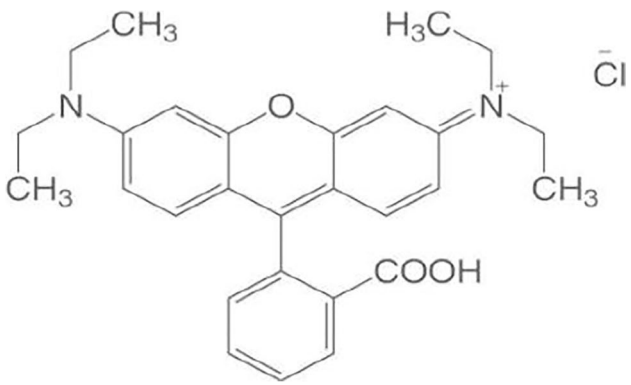

Fig. 1 Rhodamine B molecule structure

acquire 150 µm of powder size, which was the biosorbent used in the biosorption tests.

2.3 Determination of Rd-B concentration

The Rd-B dye concentration was determined with a T-60 UV–Vis spectrophotometer (China) at 558 nm [30].

2.4 Characterisation of Labada (*Rumex*).

Scanning electron microscope (SEM) (TESCAN MIRA3 XMU) equipped with energy dispersive X-ray (EDX) (TESCAN MIRA3 XMU) was used to observe the surface morphology of Labada (*Rumex*) biosorbent. A small amount of biosorbent was placed in the SEM chamber for scanning under 20 kV accelerating voltage, 2000–5000 times magnifications, and low vacuum mode. Fourier transform infrared (FTIR) spectrometer (ATR, Bruker Mode: Tensor II) was used to identify the chemical functional groups in the Labada (*Rumex*) biosorbent. Approximately, 10 mg of biosorbent was gently pressed by a stainless steel probe on the diamond holder. A spectrum range of 4000 to 400 cm^{-1} was recorded with 20 replications of scan.

2.5 Batch biosorption experiments

The bisorption of Rd-B onto Labada (*Rumex*) was investigated in the batch biosorption experiments. Analytical grade rhodamine B (Rd-B) ($C_{28}H_{30}N_2O_3$, 442.55 g/gmol) from Sigma-Aldrich was procured and utilised directly; 1000 mg L^{-1} Rd-B stock solution was prepared with dissolution of dye. The stock solution was further diluted with deionised water accordingly to obtain the desired initial concentration of rhodamine B (Rd-B) solutions. All the batch experiments were carried out 10 mL polypropylene tubes containing 100 mg Labada (*Rumex*) with constant concentration of 500 mg L^{-1} (1.04×10^{-3} mol L^{-1}) Rd-B in 10 ml solutions for 24 h at 25 °C. The effect of various parameters to the Rd-B biosorption such as initial pH:2.0–12.0; different amounts of Labada (*Rumex*) samples as 10, 30, 50, 100, 200, and 300 mg; Rd-B initial concentration: 10–1000 mg L^{-1} (0.20×10^{-4}–2.1×10^{-3} mol L^{-1}); contact time: 10–1440 min; and temperature: 5 °C, 25 °C, and 40 °C, and recovery was investigated. In the recovery study, dilute HCl, NaOH, and ethanol solutions were used for recovery of the Rd-B from the surface of the Labada (*Rumex*). After all of the each experiment, the solutions were centrifuged at 4000 rpm for 5 min, and the supernatant was then filtered and the remaining Rd-B dye concentration was determined. Biosorption%, Q (mol kg^{-1}), and % desorption were calculated with Eqs. 1, 2, and 3.

$$\text{Biosorption}\% = \left[\frac{C_i - C_f}{C_i}\right] \times 100 \tag{1}$$

$$Q = \left[\frac{C_i - C_f}{m}\right] \times V \tag{2}$$

$$\text{Desorption}\% = \frac{Q_{des}}{Q_{ads}} \times 100 \tag{3}$$

where C_i is the initial concentration (mg L^{-1}), m refers to the biosorbent mass (g), C_f is equilibrium concentration (mg L^{-1}), V is the solution volume (L), Q_{des}; desorbed amount of Rd-B dye (mol kg^{-1}) and Q_{ads}; and biosorbed amount of Rd-B dye (mol kg^{-1}).

Every experiment was repeated thrice and the average values are reported in this paper. Control tests which were identical to the biosorption experiments, but without the addition of biosorbent, were carried out concurrently to assess the loss of rhodamine B (Rd-B) due to external factors such as degradation and sorption onto glass wall.

3 Results and discussion

3.1 FT-IR and SEM–EDX analysis

FTIR was used to determine the chemical functionalities of Labada (*Rumex*) before and after the biosorption of rhodamine B (Rd-B) (Fig. 2). It provides information on the chemical groups which might be actively involved in binding the dye ions. The distinct FTIR peaks were obtained within the range of 4000 to 500 cm^{-1}. The peaks detected at 3262, 2921, 1606, 1442, 1318, 1208, 1028, 762, and 510 cm^{-1} were associated with the stretching of –OH in hydroxyl group, C–H stretching in methyl and methylene groups, C=C stretching in α,β-unsaturated ketone, O–H bending in carboxylates, O–H bending in phenol group, S=O sulfur-containing compounds, C–O bond in carboxylic acid, and C–H bend, correspondingly (Arslanoğlu). Some changes on the peaks were observed after the biosorption of rhodamine B. The overall intensities of the peaks decreased with several shifts of peaks such as from 3262 to 3275 cm^{-1}, 1208 to 1210 cm^{-1}, and 1028 to 1026 cm^{-1}. These changes implied that hydroxyl, carboxylic, and sulphonate groups were involved in the biosorption of rhodamine B (Rd-B) through adsorption. The SEM–EDX and FTIR analyses presented consistent findings which supported the involvement of adsorption mechanism in the biosorption of rhodamine B (Rd-B) [25, 29].

SEM was used to examine the surface morphology of Labada (*Rumex*) biosorbent, and the results indicated that the biosorbent had a rough surface packed with numerous

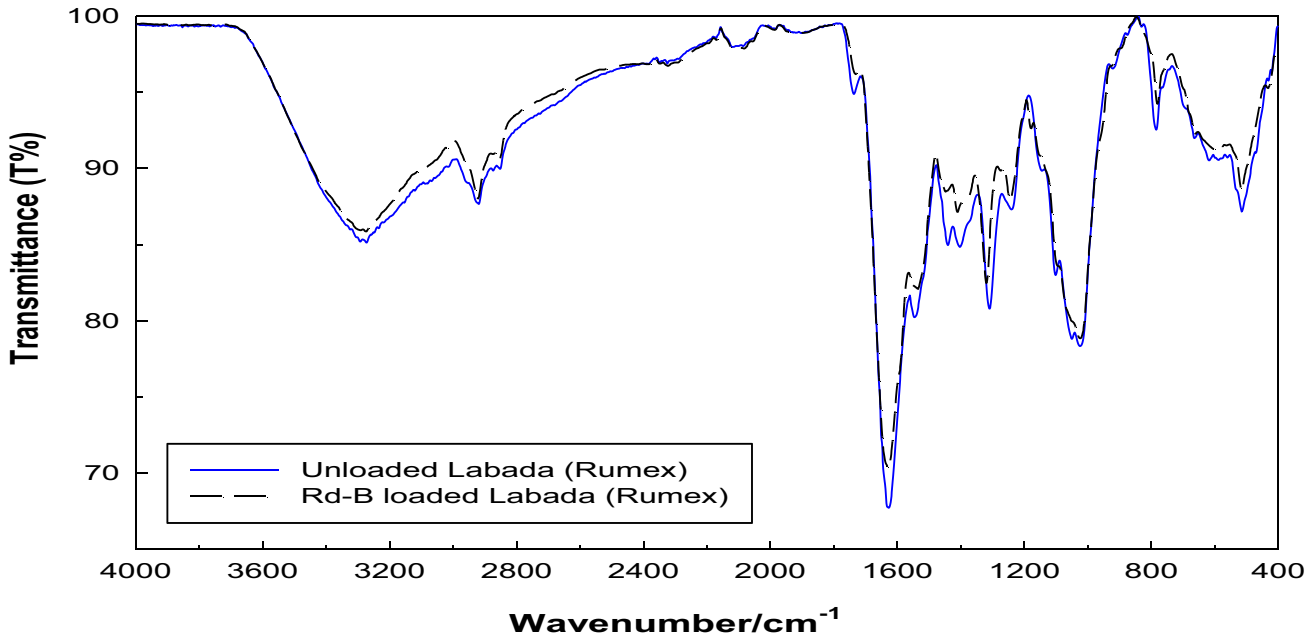

Fig. 2 FT-IR spectrum of unloaded and Rd-B loaded Labada (Rumex)

asymmetrical voids and cavities (see Fig. 3). These coarse features of Labada (*Rumex*) surface might possibly act as the binding sites for the uptake of rhodamine B (Rd-B) through pore adsorption. The SEM micrograph after rhodamine B (Rd-B) biosorption demonstrated that the biosorbent surface had become relatively smoother with the presence of spots. As suggested by Arslanoğlu [2], the spots might be the dye ions deposited on the biosorbent surface. Meanwhile, the EDX diagram portrays the elemental compositions of Labada (*Rumex*) before and after the biosorption of rhodamine B (Rd-B) (see Fig. 3). The main biosorbent constituents were carbon and oxygen which were not affected much by the biosorption. After biosorption, the peaks of potassium (K) disappeared, which might be due to the interaction with rhodamine B (Rd-B) through mechanisms such as ion-exchange. This finding was supported by the new rhodamine B (Rd-B) peaks detected around 2 keV which implied the replacement of K originally present by Rhodamine B (Rd-B) [34].

3.2 Effect of inital pH and PZC for Labada (*Rumex*).

The pH of the solution has a significant effect on the solubility of the dye ions and the adsorption process. The effect of solution pH on the amount of dye ions removed from the aqueous solution with Labada (Rumex) is shown in (Fig. 4). As the pH of the dye ion solution decreases, the amount of biosorption of Rd-B ions increases. This is probably due to the presence of few H^+ ions at low pH that compete with Rd-B ions for the active sites of Labada (Rumex). The reduction in biosorption efficiency at high pH is mainly due to the formation of soluble hydroxyl complexes [32]. To prevent the formation of these complexes, all experiments were performed at a natural solution pH of 5.5–6. As a result of the experiments, it was calculated that the biosorption capacity varies between 0.7 and 0.58 mol kg^{-1}.

Particles biosorb ions in the dispersion medium. They are positively and negatively charged. According to the positive and negative charge of each particle, they can hold the opposite ions. A monolayer (monomolecules) structure is formed. Around this layer, there is a second mobile ion layer, which is not bound to particles. This layer is called the Helmholtz bilayer or the mobile diffused bilayer. The potential of the electrical layer adhered to the particle surface is called the electrothermodynamic potential or the Nernst potential. Outside the double layer, there is a neutral field where positive ions are equal to negative ions. The potential difference between the surface of the particle and this neutral zone is called the zeta potential [2].

3.3 Effect of biosorbent mass

Dosage was negatively correlated to the response of the model. Generally, Rd-B biosorption capacity decreases with increasing dosage as illustrated in Fig. 5. As the dosage increased, the occurrence of biosorbent agglomeration decreased the total amount of binding sites for dye ions. This consequently reduced the dye uptake rate. The lowest biosorption capacity of Rd-B (10.31 mg/g) was achieved at the highest biosorbent dosage of 30.0 g L^{-1} and the

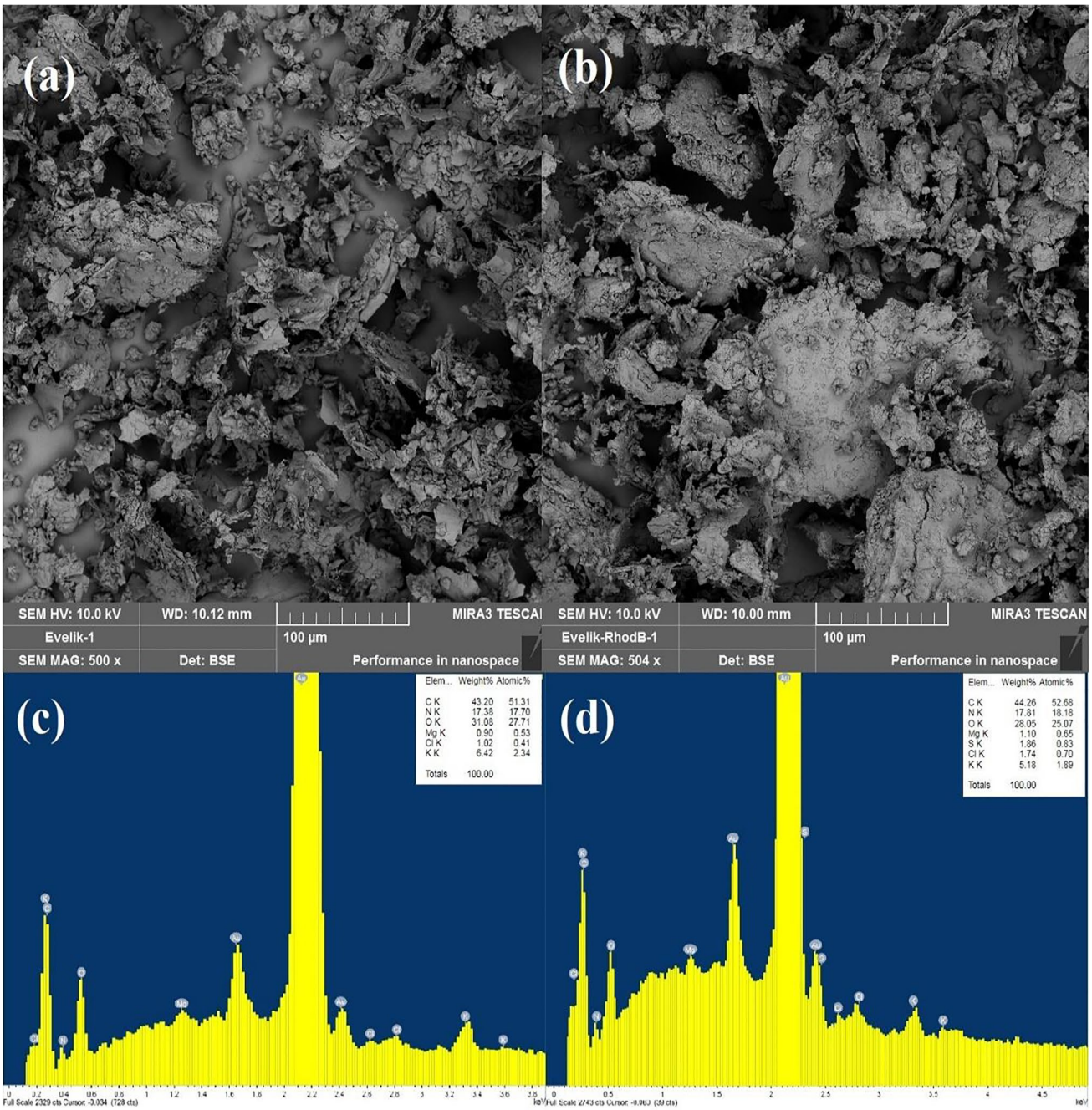

Fig. 3 SEM images of Rd-B biosorption before (a) and after (b) and EDX spectrums of Rd-B biosorption before (c) and after (d)

lowest initial Rd-B concentration. As the dosage reduced and the concentration increased, the biosorption capacity increased correspondingly. The highest biosorption capacity was achieved at 1 g L^{-1} of dosage an approximate of 0.25 mol kg^{-1}. This resulted from the desirable condition whereby high initial concentration increased the ratio of initial dye solute to the available binding sites, which consequently enhanced the driving force of Rd-B ions to promote the high removal efficiency [17].

3.4 Isotherms of biosorption process

The surface properties of the material and the interaction mechanism of the adsorption process were assessed by the Langmuir, Freundlich, and Dubinin-Radushkevich isotherm models. The Langmuir isotherm assumes that the surface of the adsorbent has a uniform and identical sites with a monolayer adsorption process. The Freundlich isotherm depicts a multilayer adsorption process on a heterogeneous surface

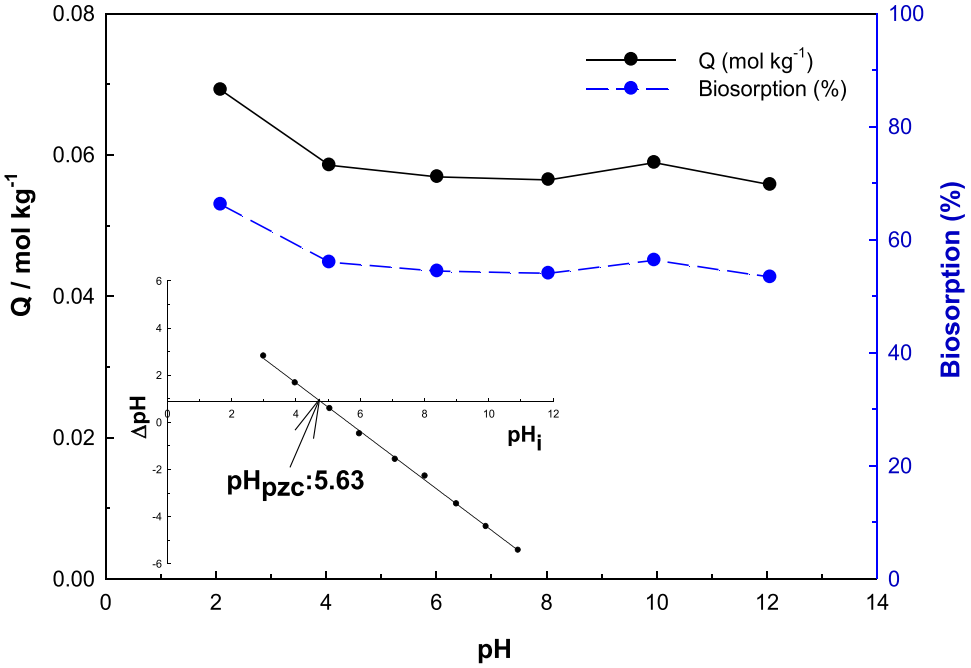

Fig. 4 Effect of pH on Rd-B biosorption onto Labada (Rumex) {[Rd-B]0:500 mg L − 1, adsorbent dosage: 100 mg, natural pH:2.0–12.0, contact time:24 h, temperature: 25 °C}

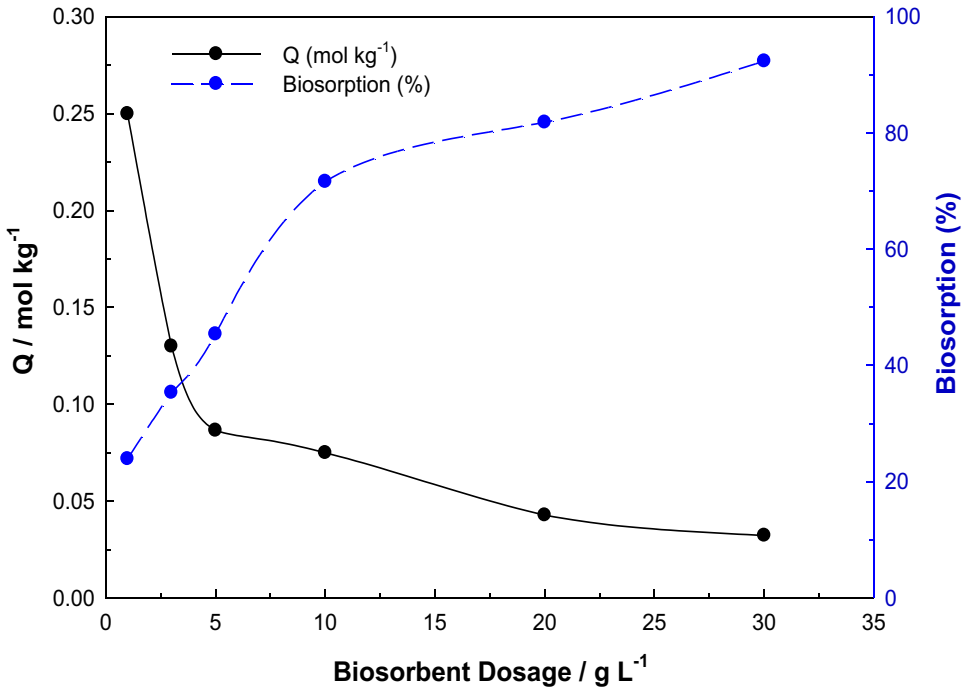

Fig. 5 Effect of biosorbent mass on Rd-B biosorption onto Labada (Rumex) biosorbent {[Rd-B]0: 500 mg L − 1, adsorbent dosage: 10, 30, 50, 100, and 200 mg, natural pH: 5.5–6.0, contact time: 24 h, temperature: 25 °C}

while the Dubinin-Radushkevich isotherm is a chemical adsorption that assumes that the heats of adsorption decrease linearly due to the interaction of the adsorbate and adsorbent across different layers of adsorption [3, 4].

To better understand the biosorption of rhodamine B (Rd-B) onto studied Labada (*Rumex*), we fitted our experimental data obtained under equilibrium conditions into several frequently used biosorption isotherms (Freundlich, Langmuir, and Dubinin-Radushkevich) (Fig. 6). The forms of these isotherms are [3, 4]:

$$Q = \frac{X_L K_L C_e}{1 + K_L C_e} \tag{4}$$

$$Q = K_F C_e^{\beta} \tag{5}$$

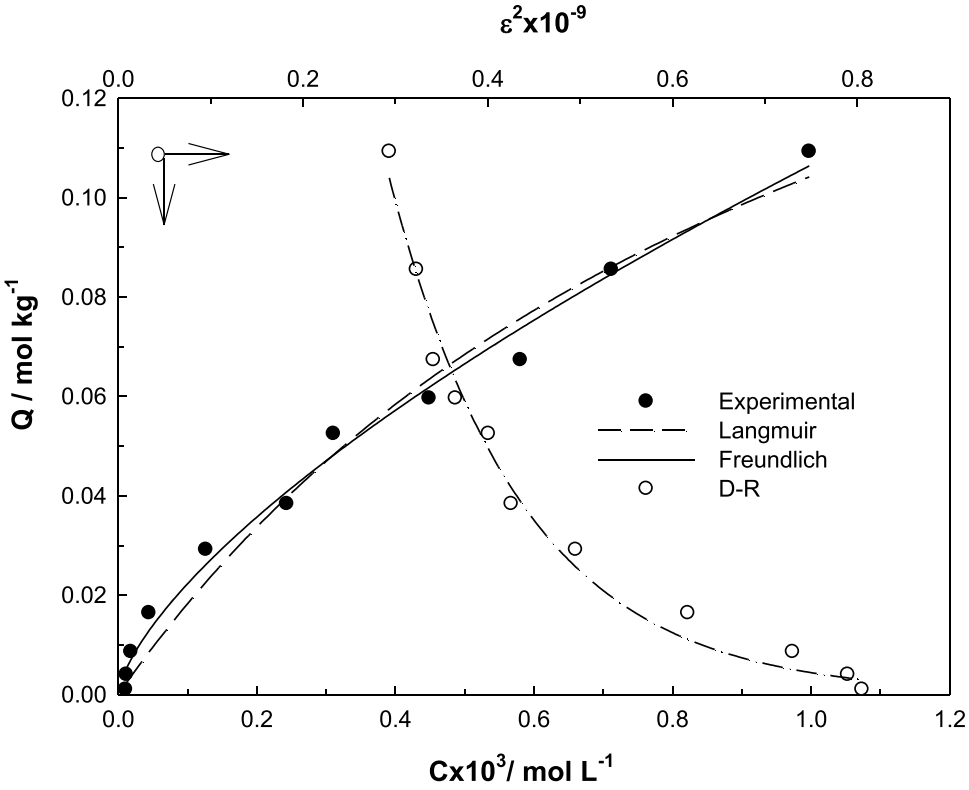

Fig. 6 Experimentally obtained adsorption isotherms Rd-B onto Labada (Rumex) and their compatibility to Langmuir, Freundlich, and D-R models {[Rd-B]0: 10–1000 mg L − 1, adsorbent dosage: 100 mg, natural pH: 5.5–6.0, contact time: 24 h, temperature: 25 °C}

$$Q = X_{DR}e^{-K_{DR}\varepsilon^2} \tag{6}$$

$$\varepsilon = RTln(1 + \frac{1}{C_e}) \tag{7}$$

$$E_{DR} = \left(2K_{DR}\right)^{-0.5} \tag{8}$$

Here X_L: the maximum biosorption capacity (mol kg^{-1}); K_L: the parameter for Langmuir isotherm; Q: the amount of biosorbed Rd-B (mol kg^{-1}); C_e: the equilibrium concentration (mol L^{-1}); X_F: Freundlich constant; β: biosorbent surface heterogeneity; X_{DR}: a measure of biosorption capacity; K_{DR}: the activity coefficient (mol^2KJ^2); ε: the Polanyi potential; R: the ideal gas constant (8.314 $Jmol^{-1}$ K^{-1}); E_{DR}: the biosorption energy (kJ mol^{-1}); and T: the absolute temperature (K), it is expressed as:

The experimental data of Rd-B biosorption onto Labada (Rumex) biosorbent were fitted non-linearly to the Langmuir, Freundlich, and D-R isotherm models in order to describe the equilibrium relationship between Rd-B and the biosorbent at constant temperature. The calculated parameters of the models are presented in Table 1. As shown in Table 1, the Langmuir model was the best-fit model with R^2 closest to unity (0.99). This suggested the occurrence of monolayer sorption of Rd-B onto the active sites of Labada (Rumex) biosorbent and that the distribution of active sites was homogeneous. Increasing q_m with increasing temperature might be explained by the endothermic nature of the process whereby the increase in mobility of the dye ions with temperature increased the rate of biosorption (Yaras and Arslanoğlu, 2018). However, the Langmuir model gives extremely high values of the maximum adsorption capacity of the monolayer (q_{max} up to 0.219 mol kg^{-1}), which is not in accordance with the literature data for dyes adsorption on carbon materials.

Table 1 Langmuir, Freundlich, and Dubinin-Radushkevich isotherm models parameters

Isotherm	Value	R^2
Langmuir		
X_L (mol kg^{-1})	0.219	0.979
K_L (L mol^{-1})	908	
Freundlich		
X_F	11.6	0.991
B	0.679	
D-R		
X_{DR} (mol kg^{-1})	0.795	0.986
$K_{DR}\times10^9$/mol^2 KJ^{-2}	6.93	
E_{DR}/kJ mol^{-1}	8.50	

3.5 Effect of contact time on biosorption

One of the important parameters in biosorption studies is the contact time between the biosorbent and the dye ions in the solution. The effect of contact time on Rd-B removal with Labada (Rumex) is shown in (Fig. 7). Biosorption was carried out at optimum pH and temperatures of 5, 25, and 40 °C by taking Rd-B solution and adsorbent. With the data obtained in a time interval of 0–1440 min, the q_e graph was plotted against time, and the equilibrium time was determined to be 240 min (Fig. 7). Rd-B removal initially showed a smooth increase up to 120 min. The reason why the increase in the removal of Rd-B ions with the increase of the biosorption time remained constant after 240 min is due to the saturation of the available areas (Yaras and Arslanoğlu, 2019).

The adsorption kinetic model was used to describe the adsorption mechanism, the diffusion phenomena, and the relationship between the equilibrium time and adsorption capacity. The model explains the efficiency and effectiveness of the adsorbent material at liquid–solid interface using the pseudo-first-order (PFO), pseudo-second-order (PSO), and intraparticle diffusion (IPD) models (Table 2).

$$Q_t = Q_e\left[1 - e^{-k_1 t}\right] \tag{9}$$

$$H_1 = k_1 Q_e \tag{10}$$

Table 2 PFO, PSO, and IPD kinetic models parameters

Kinetic model	Value	R^2
PFO		
q_t/mol kg^{-1}	0.055	0.948
q_e/mol kg^{-1}	0.052	
$k_1 \times 10^3$/dk^{-1}	45.7	
$H \times 10^3$/mol kg^{-1} min^{-1}	2.35	
PSO		
q_t/mol kg^{-1}	0.055	0.989
q_e/mol kg^{-1}	0.056	
$k_2 \times 10^3$/mol^{-1} kg min^{-1}	1131	
$H \times 10^3$/mol kg^{-1} min^{-1}	4.0	
IPD		
$k_i \times 10^3$/mol kg^{-1} min$^{-0.5}$	9.91	0.905

$$Q_t = \frac{t}{\left[\frac{1}{k_2 Q_e^2}\right] + \left[\frac{t}{Q_e}\right]} \tag{11}$$

$$H_2 = k_2 Q_e^2 \tag{12}$$

$$Q_t = k_i t^{0.5} \tag{13}$$

Here, Q_t: the biosorbed amount at time (mol kg^{-1}); Q_e: the biosorbed amount at equilibrium (mol kg^{-1}); t: time (min); k_1: the rate constant of the PFO (min^{-1}); H_1: initial biosorption rate for PFO (mol kg^{-1} min^{-1}); k_2: the rate constant of

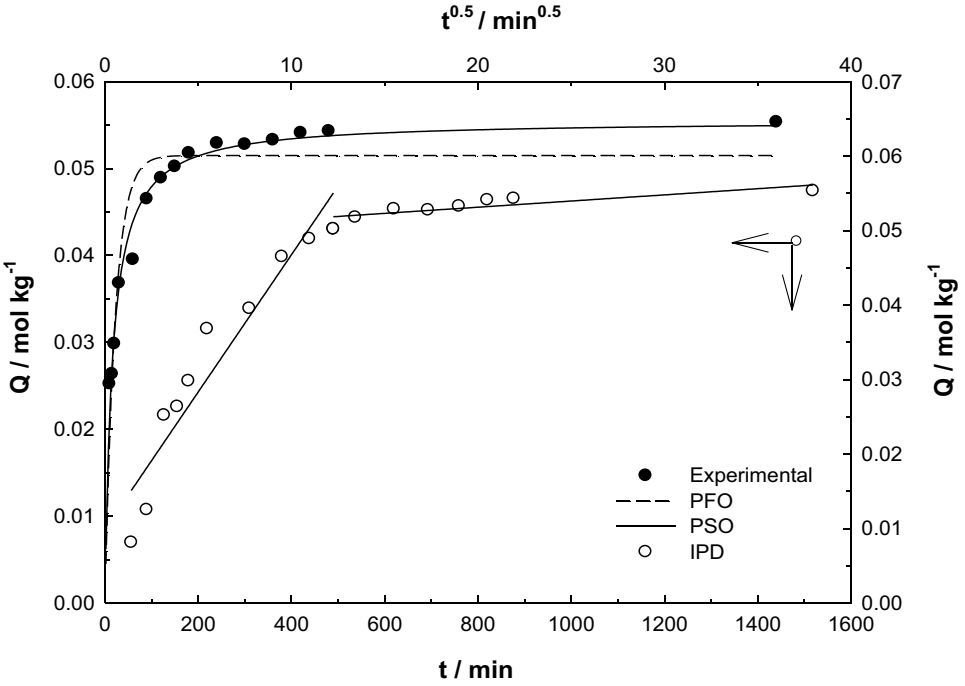

Fig. 7 Compatibility of Rd-B biosorption kinetics to PFO, PSO, and IPD models {[Rd-B]0: 500 mg L − 1, adsorbent dosage: 300 mg, natural pH: 5.5–6.0, contact time: 10–1440 min, temperature: 25 °C}

the PSO model (mol^{-1} kg min^{-1}); H_2: initial biosorption rate for PSO (mol kg^{-1} min^{-1}); and k_i: the rate constant of the IPD (mol^{-1} kg min$^{-0.5}$), and it is expressed as:

To determine the kinetics of the uptake of Rd-B, the pseudo-first-order, pseudo-second-order, and intraparticle diffusion models were fitted by the experimental data (Fig. 7). From the plots, the biosorption process could be distinguished into two stages. The initial stage was a rapid process which occurred in the first 30 min with a large fraction of Rd-B adsorbed onto the biosorbent. This was due to the abundant availability of active sites in the biosorbent. After 30 min, the second biosorption stage occurred at a lower biosorption rate attributed to the depletion of vacant sites. Equilibrium was then attained in less than 120 min when all the sorption sites of biosorbent were saturated. This was mainly due to the increased driving force of Rd-B overcoming the mass transfer limitations. Table 2 shows the calculated kinetic parameters at each concentration for the respective model.

From the R^2 value in Table 2, it could be seen that pseudo-second-order model was the best fit kinetic model. The R^2 (0.989) exhibited the closest to 1 at any fixed concentration. The good agreement with the model implied that the Rd-B uptake by PSO was mainly through chemisorption. The process might involve electron sharing or exchange between the functional groups of biosorbent and the dye ions.

3.6 Effect of temperature and adsorption thermodynamic studies

The thermodynamic parameters of the biosorption process such as enthalpy change (ΔH^0, kJ mol^{-1}), entropy change (ΔS^0, kJ mol^{-1}), and Gibbs free energy change (ΔG^0, kJ mol^{-1}) were determined by the equations below.

$$K_D = \frac{Q}{C_e} \tag{14}$$

$$\Delta G^0 = -RTlnK_D \tag{15}$$

$$lnK_D = \frac{\Delta S^0}{R} - \frac{\Delta H^0}{RT} \tag{16}$$

where R (J mol^{-1} K^{-1}) is the gas constant, T (K) is the temperature, and K_D is the distribution coefficient calculated from q_e/C_e. From the plot of lnK_D against $1/T$, the values of ΔH and ΔS can be obtained from the gradient and the intercept of y-axis, respectively (Fig. 8).

Calculating the heat of adsorption from adsorption isotherms at different temperatures or measuring it using calorimetric techniques can characterize the exothermicity of an adsorption system. There are two types of adsorption processes: physical adsorption (or physisorption) and chemical adsorption (or chemisorption) which differ in their heat of adsorption values (Eqs. 14, 15, and 16). Physisorption involves non-specific forces of the Van der Waals type; the absorption heat is estimated at 40 kJ mol^{-1}. In the case of chemisorption, the interactions are stronger, inducing a higher heat of absorption which could reach 200 kJ mol^{-1} [24].

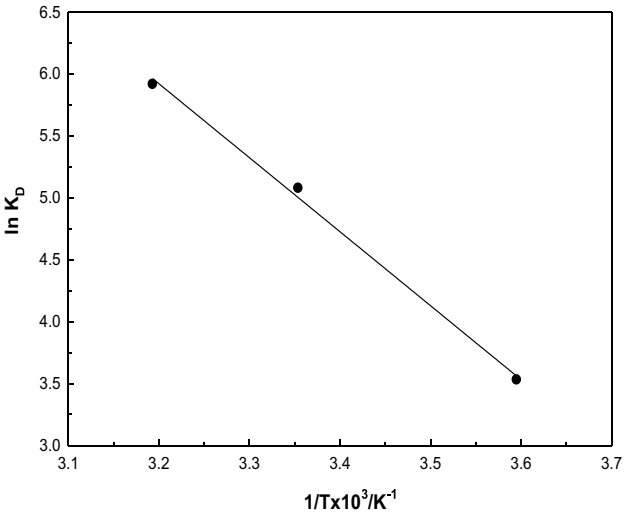

Fig. 8 The effect of temperature on the biosorption {[Rd-B]0: 500 mg L − 1, adsorbent dosage: 100 mg, natural pH: 5.5–6.0, contact time: 24 h, temperature: 5 °C, 25 °C, and 40 °C}

Table 3 Thermodynamic parameters for Rd-B biosorption by Labada (*Rumex*)

Temperature (°C)	ΔH (kJ mol^{-1})	ΔG (kJ mol^{-1})	ΔS (J mol^{-1} K^{-1})
5	39.7	− 8.18	208
25		− 12.4	
40		− 15.5	

Table 3 shows the ΔH°, ΔG°, and ΔS° values obtained from the three Van't Hoff equations. Physisorption is indicated by values of ΔH° between 1 and 40 kJ mol^{-1}. These results show that, for the biosorption of the Rd-B dye, physisorption is considerably more favourable. The Rd-B dye biosorption endothermic nature is demonstrated by positive values of ΔH°.

ΔH^0 was found as 39.7 kJ mol^{-1}, and ΔS^0 was calculated as 208 Jmol^{-1} K^{-1}. ΔG^0 was found as − 8.18 kJ mol^{-1}, − 12 .4 kJ mol^{-1}, and − 15.5 kJ mol^{-1} at 5 °C, 25 °C, and 40 °C, respectively.

On the other hand, increasing the temperature inhibits the biosorption of Rd-B dye on Labada (*Rumex*) means that the reaction is exothermic ($\Delta H^\circ < 0$). The biosorption is very favourable and spontaneous, as indicated by negative values

of ΔG°. The increased disorder and randomness at the solid solution interface of the Rd-B dye with the Labada (*Rumex*) biosorbent, as shown by the positive values of ΔS°, causes structural changes for Rd-B dye on the surface of the Labada (*Rumex*) adsorbent. The thermodynamic parameters for Rd-B dye biosorption were evaluated using isotherm experimental data at different temperatures. The parameter values obtained are listed in. The negative ΔG^0 values determined for all concentrations, and temperatures indicated that the biosorption was spontaneous with high Rd-B dye affinity to Labada (*Rumex*) biosorbent [3, 4]. Increasing negativity of ΔG^0 with increasing temperature suggested the increased feasibility of Rd-B dye biosorption at higher temperatures. The ΔS^0 values were found to be positive which suggested that the Rd-B dye uptake process increased the randomness at the solid–liquid interface. The positive ΔH^0 indicated an endothermic biosorption process in which the rate of Rd-B dye uptake increased as the temperature increased [10] (Table 3).

3.7 Biosorption mechanism

Biosorption mechanism intraparticle diffusion model was used to further investigate the rate-controlling steps in Rd-B dye uptake by Labada (*Rumex*) biosorbent using the kinetic experimental data. Generally, the transport of the dye ions from the liquid phase to the solid phase of biosorbent involves sequential biosorption mechanisms such as boundary layer diffusion, intraparticle diffusion, and surface sites sorption. The rate-limiting step of the overall biosorption process can be governed by a single or multiple mechanisms [23]. The q_t versus $t^{0.5}$ plot at 20, 40, 60, 80, and 100 mg L^{-1} are illustrated in Fig. 3c, and the calculated k_p and *y*-intercept (C) are shown in Table 3. If the plots were extrapolated to the *y*-axis, none of the plots would pass through the origin. This implied that the biosorption process not only involved intraparticle diffusion, but also several steps such as diffusion through the boundary layer. The calculated *y* intercept indicates the thickness of the boundary layer of biosorbent. A large intercept represents a thick boundary layer which results in the increment of boundary layer effect. As shown in Fig. 3c and Table 3, the *y*-intercept increased with initial concentration, suggesting the increase in boundary layer thickness. Hence, the boundary effect of the biosorption process was greater at a higher initial concentration [31].

In the peak aliphatic –CH3, $=CH_2$ groups at FTIR 2900 cm^{-1} showed asymmetric CH stretching of the 1720 cm^{-1} hemicellulose C = O stretching vibration. The 1625 cm^{-1} stretch vibration of lignin's carbonyl groups represented the C = O bond and 1510 cm^{-1} shows the stretching vibration of ethylene (–C = C–) in the aromatic ring structure of lignin. The 1440 cm^{-1} aliphatic ($–CH_3$) group refers to the C–H deformation vibration originating from the aliphatic parts of the lignin. Other peaks are in 1390 cm^{-1} structure; aliphatic C–H bending vibration of methyl and phenyl alcohols, 1259 cm^{-1}; C–O stretching vibration in the ring structure of lignin and xylene, 128 cm^{-1}; representing the C–OH stretching vibration of cellulose and hemicellulose. The 875 cm^{-1} peak was due to the out-of-plane aromatic C–H stretching vibration. This shows that Labada (Rumex), which is predominantly cellulose and hemicellulose (Table 4), has an active adsorbent structure (Fig. 9).

3.8 Comparison of adsorbents studied in the literature

The rapid removal of Rd-B dye is essential in the adsorption process practice as it will promote the use of treated Labada (*Rumex*) for efficiency and economy. The adsorption capacity is in the order of 0.219 mol kg^{-1} for Rd-B dye with optimal conditions of Rd-B: 100 mg L^{-1}, biosorbent dose: 1 g L^{-1}, and natural solution pH of 5.5–6.0. The maximum adsorption capacities of treated Labada (*Rumex*) for the Rd-B dye were compared in terms of optimal conditions, adsorption mechanism, and adsorption patterns with different types of adsorbents which have been reported and documented in the scientific literature as shown in Table 5. Unlike other adsorbents, the Labada (*Rumex*) material can be considered a cost-effective and fast alternative: some adsorbents might have higher adsorption power, but their adsorption process takes a long time. Besides, due to its good adsorption capacities obtained, Labada (*Rumex*) is a promising adsorbent for the treatment of cationic Rd-B dye which is known by the difficulty of its removal from aqueous solutions. From our results obtained, we have found very high adsorption capacities similar to those obtained by other authors who have worked on the adsorption of cationic dyes by adsorbent materials based on wheat flour.

3.9 Desorption study results

The economic and environmental implications of the biosorbent material used lead to significant reuse of treated Labada (*Rumex*) due to its low cost and regeneration potential. The regeneration experiments were carried out after pores saturation with the biosorbent Labada (*Rumex*) (1 g

Table 4 Physicochemical characteristic properties of Labada (*Rumex*)

Chemical analysis	Value wt (%)
Extractive matters	12.4
Hemicellulose	20.8
Cellulose	15.6
Lignin	1.14
Ash	0.5

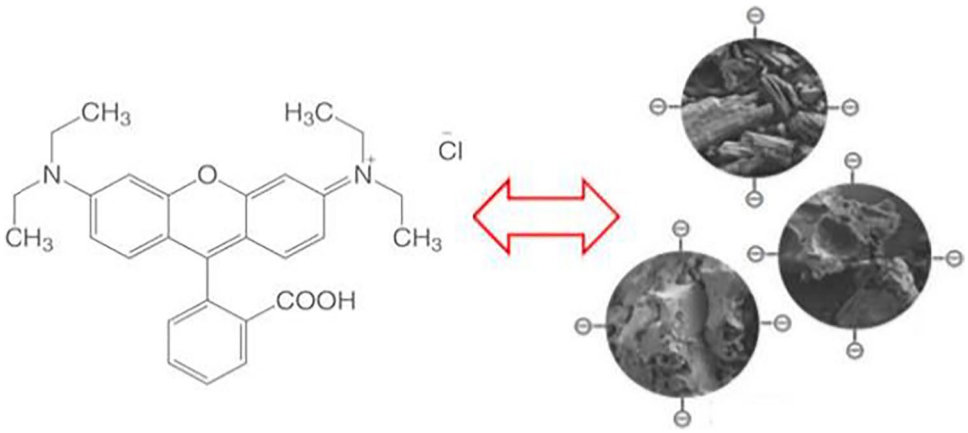

Fig. 9 Biosorption mechanism demonstration of RdB by Labada (Rumex)

Table 5 Comparison of sorption capacities of different adsorbents for Rd-B removal

Adsorbent	Sorption capacity (mg/g)	References
Rhizopus oryzae biomass	39.21	Das et al. [8]
Bagasse pith	21.5	Gad and El-Sayed [11]
Treated parthenium biomass	59.2	Lata et al. [19]
Coir pith	2.6	Namasivayam et al. [22]
Poly(glutamic acid)	390.2	Inbaraj et al. [14]
Carbonaceous adsorbent	82.8	Bhatnagar and Jain [6]
Labada (*Rumex*)	104.9	This study

L^{-1}) with the dye Rd-B at a concentration of 100 mg L^{-1}. The desorption experiments were all carried out using different solvents, such as distilled water, NaOH (%20), HCl (%50), and ethanol (%18). Figure 10 shows that HCl solutions gave good desorption results compared to other solvents (NaOH and ethanol) which approach 50% Rd-B dye. In our study, we obtained similar results to the work of some researchers who worked on thermal regeneration as well as solvent regeneration of Labada (*Rumex*). Furthermore, the adsorption process on an industrial scale depends essentially on the adsorbent regeneration capacity at a cheaper cost [12].

3.10 Cost analysis of Labada (*Rumex*) used for biosorption

The competitive industrial aspect of low-cost adsorbent materials remains the main objective of many researchers when dealing with textile pollutants. Cost analysis study is a very important parameter to evaluate and estimate the price of our Labada (*Rumex*) adsorbent material and to give the possibility to compare this adsorption study with another

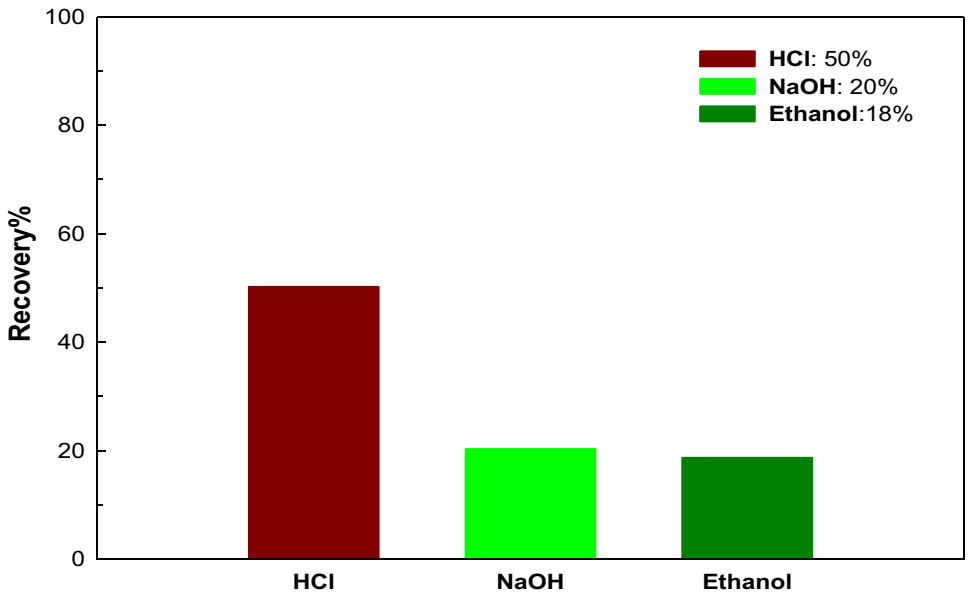

Fig. 10 The effect of recovery for Labada (Rumex) {[Rd-B]0: 500 mg L – 1, adsorbent dosage: 100 mg, natural pH: 5.5–6.0, contact time: 24 h, temperature: 25 °C}

method of textile pollutants treatments. Moreover, according to in-depth bibliographical research, it is noted that this study of estimating the adsorbent cost has never been applied in the adsorption field. In addition, our study is based on the unit price of treated Labada (*Rumex*) adsorbent materials used after treatment. It can be seen that the estimated price of our Labada (*Rumex*) adsorbent material to be around $ 0.8 for 1 kg of adsorbent for treated of Rd-B dye. From these cost results, our material can be considered to be a low-cost adsorbent [13].

4 Conclusion

The treated Labada (*Rumex*) adsorbent has been prepared and characterized by a sequential and methodical approach to understanding the surface morphology, porosity, and selectivity of the material for good and rapid retention of the Rd-B dye. The removal of Rd-B dye is rapid with equilibrium adsorption capacity in the order of 109.4 mg g^{-1}. However, the equilibrium data modelling by adsorption isotherms fits with the Langmuir model, and the adsorption kinetics is best presented by a PSO model. The performance of Labada (*Rumex*) for the removal of Rd-B dye from the aqueous solution was modelled which resulted in percentage of elimination equivalent to 58%. In addition, regeneration by solvents gives us important results which explain that our Labada (*Rumex*) material is reversible and reusable after several regeneration cycles. The cost analysis shows that Labada (*Rumex*) is inexpensive and is estimated to cost around $ 0.8 per 1 kg. Overall, these results clarified that our Labada (*Rumex*) adsorbent is potential and exhibits a good specific surface area leading to a very high adsorption capacity compared to other adsorbents found in the scientific literature. Therefore, it could be considered selective, economical, and environmentally friendly for the textile dyes removal. In perspective, this study could pave the way for the industrial use of the Labada (*Rumex*) material in the preparation of beads for continuous adsorption and the development of tubular or flat-sheet membranes for the filtration of water contaminated by textile dyes.

Author contribution Zeynep Mine Şenol: conception and design of study, acquisition of data, drafting the manuscript, approval of the version of the manuscript to be published, review, and editing. Serap Çetinkaya: conception and design of study, analysis of data, drafting the manuscript, approval of the version of the manuscript to be published. Hasan Arslanoğlu: writing, analysis of data, revising the manuscript critically for important intellectual content, approval of the version of the manuscript to be published.

Data availability The data that support the findings of this study are available from the corresponding author, upon reasonable request.

Declarations

Conflict of interest The authors declare no competing interests.

References

1. Anandhan M, Prabaharan T (2018) Environmental impacts of natural dyeing process using pomegranate peel extract as a dye. Int J Appl Eng Res 13:7765–7771
2. Arslanoğlu H (2021) Production of low-cost adsorbent with small particle size from calcium carbonate rich residue carbonatation cake and their high performance phosphate adsorption applications. J Market Res 11:428–447
3. Arslanoğlu H, Kaya S, Tümen F (2020) Cr (VI) adsorption on low-cost activated carbon developed from grape marc-vinasse mixture. Part Sci Technol 38(6):768–781
4. Arslanoğlu H, Orhan R, Turan MD (2020) Application of response surface methodology for the optimisation of copper removal from aqueous solution by activated carbon prepared using waste polyurethane. Anal Lett 53(9):1343–1365
5. Azbar N, Yonar T, Kestioglu K (2004) Comparison of various advanced oxidation processes and chemical treatment methods for COD and color removal from a polyester and acetate fiber dyeing effluent. Chemosphere 55(1):35–43
6. Bhatnagar A, Jain AK (2005) A comparative adsorption study with different industrial wastes as adsorbents for the removal of cationic dyes from water. J Colloid Interface Sci 281(1):49–55
7. Bilal M, Iqbal HM, Barceló D (2019) Persistence of pesticides-based contaminants in the environment and their effective degradation using laccase-assisted biocatalytic systems. Sci Total Environ 695:133896
8. Das SK, Bhowal J, Das AR, Guha AK (2006) Adsorption behavior of rhodamine B on rhizopus o ryzae biomass. Langmuir 22(17):7265–7272
9. Daştan T, Saraç H (2018) Determination of the nutritional element concentrations of Evelik plant (Rumex crispus L). Cumhuriyet Sci J 39(4):1020–1024
10. El Haddad M, Mamouni R, Saffaj N, Lazar S (2016) Evaluation of performance of animal bone meal as a new low cost adsorbent for the removal of a cationic dye rhodamine B from aqueous solutions. J Saudi Chem Soc 20:S53–S59
11. Gad HM, El-Sayed AA (2009) Activated carbon from agricultural by-products for the removal of rhodamine-B from aqueous solution. J Hazard Mater 168(2–3):1070–1081
12. Haldorai Y, Shim JJ (2014) An efficient removal of methyl orange dye from aqueous solution by adsorption onto chitosan/MgO composite: a novel reusable adsorbent. Appl Surf Sci 292:447–453
13. Hynes NRJ, Kumar JS, Kamyab H, Sujana JAJ, Al-Khashman OA, Kuslu Y and Suresh B (2020) Modern enabling techniques and adsorbents based dye removal with sustainability concerns in textile industrial sector-a comprehensive review. J Clean Prod 122636, 272:1–17
14. Inbaraj BS, Chien JT, Ho GH, Yang J, Chen BH (2006) Equilibrium and kinetic studies on sorption of basic dyes by a natural biopolymer poly (γ-glutamic acid). Biochem Eng J 31(3):204–215
15. Inoue M, Okada F, Sakurai A, Sakakibara M (2006) A new development of dyestuffs degradation system using ultrasound. Ultrason Sonochem 13(4):313–320
16. Kapdan IK, Kargi F (2002) Simultaneous biodegradation and adsorption of textile dyestuff in an activated sludge unit. Process Biochem 37(9):973–981
17. Kaur K, Jindal R (2018) Synergistic effect of organic-inorganic hybrid nanocomposite ion exchanger on photocatalytic

degradation of rhodamine-B dye and heavy metal ion removal from industrial effluents. J Environ Chem Eng 6(6):7091–7101
18. Kaur S, Rani S, Mahajan RK, Asif M, Gupta VK (2015) Synthesis and adsorption properties of mesoporous material for the removal of dye safranin: kinetics, equilibrium, and thermodynamics. J Ind Eng Chem 22:19–27
19. Lata H, Mor S, Garg VK, Gupta RK (2008) Removal of a dye from simulated wastewater by adsorption using treated parthenium biomass. J Hazard Mater 153(1–2):213–220
20. Mahmoodi NM, Hayati B, Arami M, Lan C (2011) Adsorption of textile dyes on Pine Cone from colored wastewater: kinetic, equilibrium and thermodynamic studies. Desalination 268(1–3):117–125
21. Muhd Julkapli N, Bagheri S, and Bee Abd Hamid S (2014) Recent advances in heterogeneous photocatalytic decolorization of synthetic dyes. The Scientific World Journal, 692307, 1–26
22. Namasivayam C, Radhika R, Suba S (2001) Uptake of dyes by a promising locally available agricultural solid waste: coir pith. Waste Manage 21(4):381–387
23. Nooney RI, Thirunavukkarasu D, Chen Y, Josephs R, Ostafin AE (2002) Synthesis of nanoscale mesoporous silica spheres with controlled particle size. Chem Mater 14(11):4721–4728
24. Nuhnen A, Janiak C (2020) A practical guide to calculate the isosteric heat/enthalpy of adsorption via adsorption isotherms in metal–organic frameworks MOFs. Dalton Trans 49(30):10295–10307
25. Priya MS, Divya P, Rajalakshmi R (2020) A review status on characterization and electrochemical behaviour of biomass derived carbon materials for energy storage supercapacitors. Sustainable Chemistry and Pharmacy 16:100243
26. Sarayu K, Sandhya S (2012) Current technologies for biological treatment of textile wastewater–a review. Appl Biochem Biotechnol 167(3):645–661
27. Seyrek EŞ, Yalcin E, Yilmaz M, Kök BV, Arslanoğlu H (2020) Effect of activated carbon obtained from vinasse and marc on the rheological and mechanical characteristics of the bitumen binders and hot mix asphalts. Construction and Building Materials 240:117921
28. Sezer GG, Yeşilel OZ, Şahin O, Arslanoğlu H, Erucar I (2017) Facile synthesis of 2D Zn (II) coordination polymer and its crystal structure, selective removal of methylene blue and molecular simulations. J Mol Struct 1143:355–361
29. Ţucureanu V, Matei A, Avram AM (2016) FTIR spectroscopy for carbon family study. Crit Rev Anal Chem 46(6):502–520
30. Tüzen M, Sarı A, Saleh TA (2018) Response surface optimization, kinetic and thermodynamic studies for effective removal of rhodamine B by magnetic AC/CeO2 nanocomposite. J Environ Manage 206:170–177
31. Wu FC, Tseng RL, Juang RS (2009) Initial behavior of intraparticle diffusion model used in the description of adsorption kinetics. Chem Eng J 153(1–3):1–8
32. Yaraş A, Arslanoğlu H (2019) Utilization of paper mill sludge for removal of cationic textile dyes from aqueous solutions. Sep Sci Technol 54(16):2555–2566
33. Yaraş A, and Arslanoğlu H (2018) Efficient removal of basic yellow 51 dye via carbonized paper mill sludge using sulfuric acid. Sigma J Eng Nat Sci 36(3):803–818
34. Zheng JC, Feng HM, Lam MHW, Lam PKS, Ding YW, Yu HQ (2009) Removal of Cu (II) in aqueous media by biosorption using water hyacinth roots as a biosorbent material. J Hazard Mater 171(1–3):780–785